Numerical modeling of combined reinforcement concrete beam

Ravshanbek Mavlonov*, and *Sobirjon* Razzakov

Namangan Engineering Construction Institute, Namangan, Uzbekistan

Abstract. Because polymer-composite reinforcements are a new material in construction, the possibilities of their use in load-bearing structures, including concrete beams, are somewhat limited by existing regulations. The research work implemented in this article is to study their strength and stiffness in cases where steel reinforcement is in the tensile zone and composite polymer reinforcement is in the compressive zone of concrete. Concrete beams with combined reinforcement are the object of the study, and the study of the stress-deformation state is its subject. The behavior of concrete beams with combined reinforcement under static load was studied. Considering the nonlinear properties of materials in the finite element method, their stress-strain states were investigated. A 3D beam model was created using the ANSYS Workbench 2022R1, and 3 series of samples were chosen and compared with hand calculations. The behavior of concrete beams with metal and composite reinforcement was carried out using numerical analysis. Also, the study's results show that the role of the reinforcement installed in the compressive zone of the beam is better than the performance of the beam without the reinforcement installed in the compressive zone. Although the failure starts with the rebar in the tensile zone, the rebar installation in the compression zone shows an increase in the bearing capacity and stiffness of the beam.

1 Introduction

In recent years, the increased need for metals in construction has led to tasks such as saving them and finding and searching for alternatives. Because their reserves are also decreasing, and at the same time, reserves are limited. Replacing steel reinforcement with alternative options in construction requires special attention nowadays. Today, there are also opportunities to reduce steel consumption by using composite polymer reinforcements in concrete structures instead [1, 4]. Based on ShNQ 2.03.14-18 (Uzbekistan), there are certain restrictions on using composite polymer reinforcements in load-bearing structures, mainly due to their low elastic modulus and fragility. For this purpose, we researched reducing steel rebar by using composite polymer reinforcement instead of steel reinforcement in the compression zone while keeping the steel reinforcement located in the tensile zone in the concrete beam.

* Corresponding author: ravshanbek.mavlonov@gmail.com

Because the performance of composite polymer reinforcements differs from steel, concrete beams with combined reinforcements were experimentally studied. As we know, the stress-strain behavior of steel under load obeys Hooke's law and has characteristics such as yield strength and ultimate strength. However, the yield strength is almost unobserved in composite polymer reinforcements; their diagram remains linear before rupture. In the research presented in this article, basalt composite reinforcements were used as composite polymer reinforcements together with steel for concrete beams [2, 5].

Nevertheless, FRPs exhibited brittle behavior and were characterized by their linear-elastic stress-strain response without any obvious yield point. Therefore, FRP bars do not appear ductile like steel reinforcing bars. Furthermore, there is another drawback was pointed through structural engineering viewpoint such as low modulus of elasticity and low shear strength which cause limited application for FRP bars; consequently, concrete beams reinforced with FRP bars show linear-elastic behavior up to failure without display any yield and their final failure is characterized as brittle whether it happens due to FRP rupture or due to concrete crushing; while the latter one can be considered as more advisable for RC flexural structural elements with FRPs [2,7,8].

We know that basalt fiber reinforcements have several advantages over steel. Basalt bars are less than about 25% the weight of steel rebar, greater than twice the tensile strength of steel, is electrically non-conductive, non-magnetic, insulates against thermal transfer, and of the same thermal coefficient expansion as concrete [1,4,9,12,13]. It should be noted that the data obtained from the results of experimental research are important and widely used in calculating concrete structures. There are also some negative aspects of those studies, including the fact that they require a lot of work, the costs increase due to many tests, and the presence of aspects such as the need for a long period.

Recently, a lot of experimental research has been conducted to investigate the behavior of concrete beams reinforced with FRP beams. Particularly for FRP, It has been reported that FRP-reinforced beams experience higher deflections and larger crack widths when compared to traditionally reinforced beams with steel bars [9,10,15,21]. In addition, low post-cracking and flexural stiffness have been exhibited with these beams. This is due to the low modulus of elasticity FRP which can be concluded that the behavior of reinforced concrete beams reinforced with FRP bars under different types of loads needs to investigate with analytical, experimental, and numerical research.

One of the most convenient methods for studying them and analyzing the performance of structures under load is the finite element method. Modeling structure using the finite element method allows determining the state of stress-deformability, considering both geometrically complex structures and nonlinear properties of materials. The main goal of our research is to determine the value of the destructive force and deflection, the load-bearing capacity of combined reinforced concrete beams, and to study the stress-strain states under the load with reliable results based on scientific research. The analysis of combined reinforced concrete beam was modeled using ANSYS Workbench 2022R1 nonlinear finite element software. Model components received throughout the current study, corresponding FE representation, and corresponding elements designation in ANSYS are considered the nonlinear constitutive law of each material was also implemented in the model.

The results were compared with the values based on hand calculations and experimental studies, and important practical scientific results were obtained.

2 Methods

In order to accurately modeling all components of the concrete beam, steel bars, BFRP bars, and stirrups were considered and simulated properly. Meanwhile, material properties,

nonlinear boundary conditions, and element meshing were concentrated inbuilt the model to get accurate results. The simulated models have been used as the experimental model of concrete beams. Every reinforced concrete specimen has the same amount of reinforcement, a diameter of bars, and grades of concrete compressive strength except Series 1.

The purpose of the research work is to determine the stress-strain state of concrete beams with combined reinforcement. A total of 3 series of samples were modeled in ANSYS. Results were also compared with regular steel reinforcement beams to study the stress-strain state of combined reinforced beams. It should be noted that only steel reinforcement is used in this case. The geometric dimensions of the beam and used reinforcement bars are shown in Table 1.

Table 1. The dimensions of the samples selected for the experiment and the parameters of the reinforcement bars

Samples	Sample dimensions, mm			Effective length, mm	Rebar in tension	Rebar in compression
	Length	Height	Width			
Series 1	1500	180	120	1440	2Ø12 A400	-
Series 2					2Ø12 A400	2Ø8 A400
Series 3					2Ø12 A400	2Ø8 BFRP

For Series 1, 2Ø12 A400 rebars were used in the tensile zone of the beam; for Series 2, 2Ø12 A400 in the tensile zone and 2Ø8 A400 in the compressive zone, for Series 3, 2Ø12 A400 in the tensile zone and 2Ø8 BFRP rebars were used in the compressive zone.

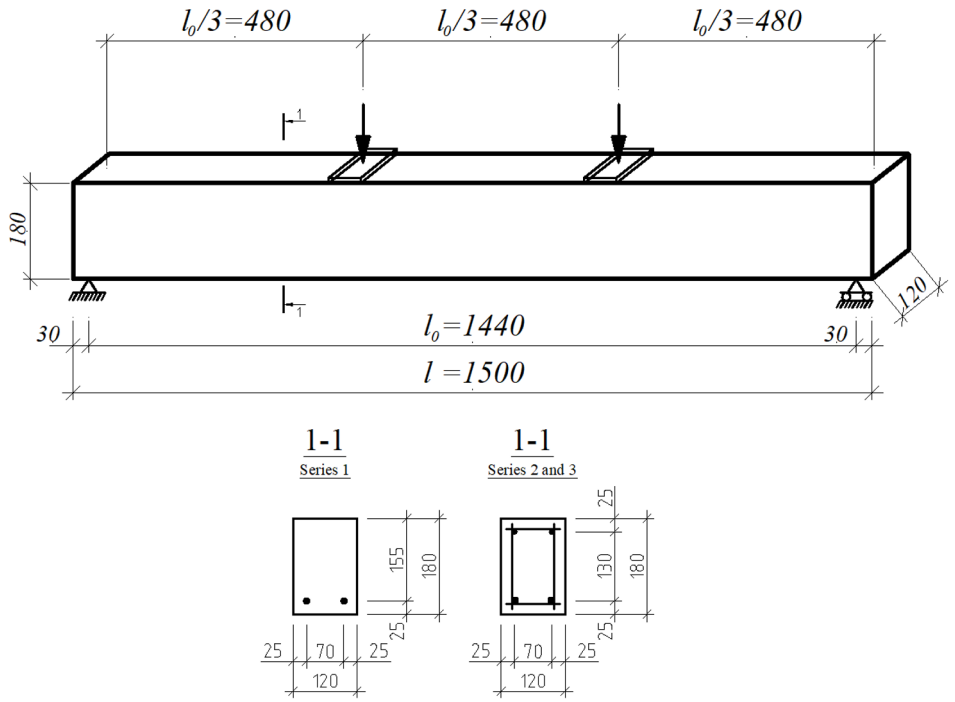

Fig. 1. 3D view and cross-section of beam

All beams were tested under four-point bending over a simply supported clear span of 1500 mm. The distributive girders were used to apply symmetric and simultaneous load at two loading points, forming a pure bending section in the midspan of the test beam. The loading pattern of the beam is shown in Fig. 1, and the reinforcement cage is presented in Fig. 2.

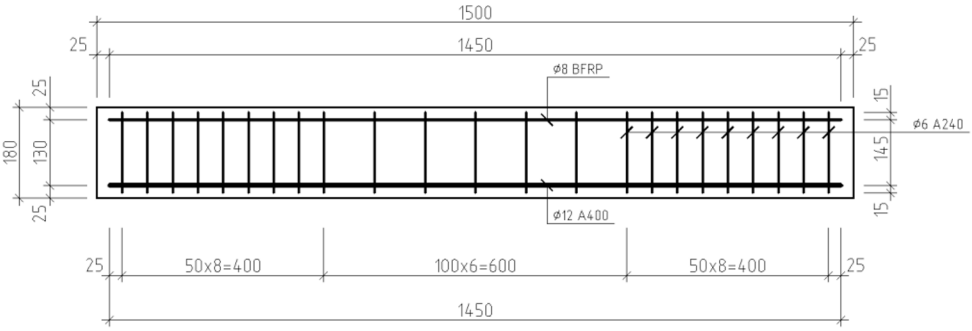

Fig. 2. Reinforcement cage of beam for Series 3

3-D eight-node CPT215 function was used for modeling in ANSYS 2022R1 software, taking into account the nonlinear properties of all materials are shown in Fig. 3. Nonlinear properties of concrete were determined using the Drucker-Prager method, Table 2.

Table 2. Drucker-Prager model for nonlinear properties of concrete

Parameter	Symbol	Value	Units
Modulus of elasticity	E	21019	MPa
Poisson's ratio	μ	0.2	
Uniaxial compressive strength	f_{uc}	20	MPa
Biaxial compressive strength	f_{bc}	23	MPa
Uniaxial tensile strength	f_{ut}	1.81	MPa
Tension cap hardening factor	R_t	1	-
Hardening parameter	D	30000	MPa^2
Compression cap location	σ^c_v	-15.33	MPa
Compression cap shape	R	2	-
Threshold for tension damage	γ_{t0}	0	-
Threshold for compression damage	γ_{c0}	0.00002	-
Tension damage parameter	β_t	3000	-
Compression damage parameter	β_c	2000	-
Nonlocal interaction range parameter	c	1600	mm^2
Over nonlocal parameter	m	2.5	-

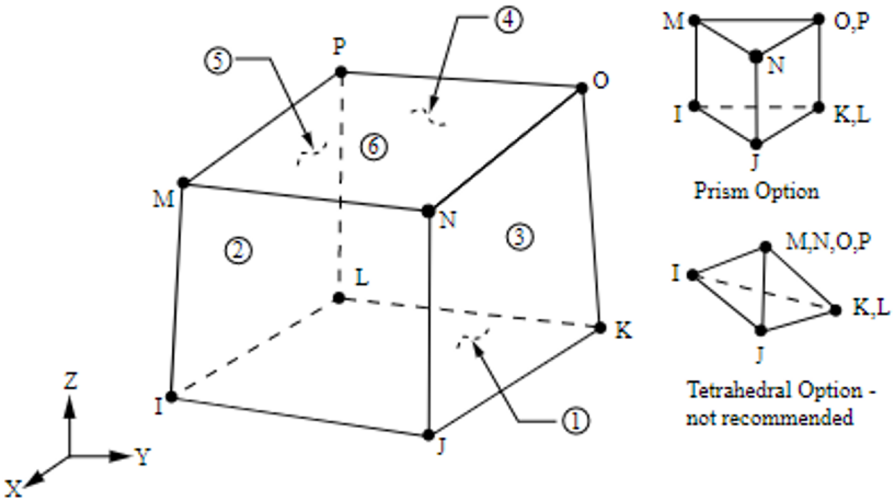

Fig. 3. CPT215 Structural Solid Geometry

In Table 3, both steel and BFRP rebar parameters are shown. For the tension zone of concrete A400 steel rebar, for compression, is BFRP bar is used.

Table 3. Characteristics of Steel and BFRP rebars

A400 steel grade parameters			**BFRP parameters**		
Parameter	**Value**	**Units**	**Parameter**	**Value**	**Units**
Modulus of elasticity	200000	MPa	Modulus of elasticity	50000	MPa
Poisson's ratio	0.3	-	Poisson's ratio	0.22	-
Tensile yield strength	365	MPa	Tensile yield strength	-	-
Compressive yield strength	365	MPa	Compressive yield strength	-	-
Tensile ultimate strength	590	MPa	Tensile ultimate strength	550	MPa
Compressive ultimate strength	400	MPa	Compressive ultimate strength	200	MPa

3 Results and discussion

According to the results, stresses and deflections in concrete and reinforcement were determined in all 3 series of samples. When the applied load is 45 kN for series 1, tensile rebar reaches its yield strength $\sigma_s=R_s=365$ MPa, as shown in Fig. 4. The failure of the beam begins in the tensile zone, and the stresses of concrete in the compressive zone reach their maximum value at the point of loading which are equal to 14.76 MPa, Fig. 5.

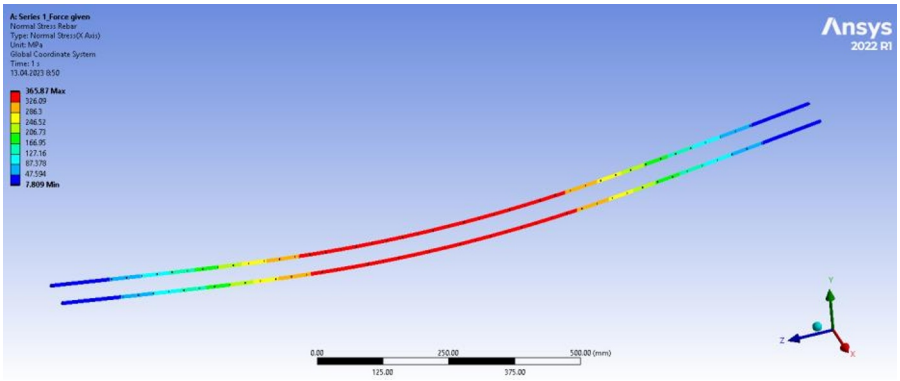

Fig. 4. Variation ranges of rebar stresses for Series 1, MPa

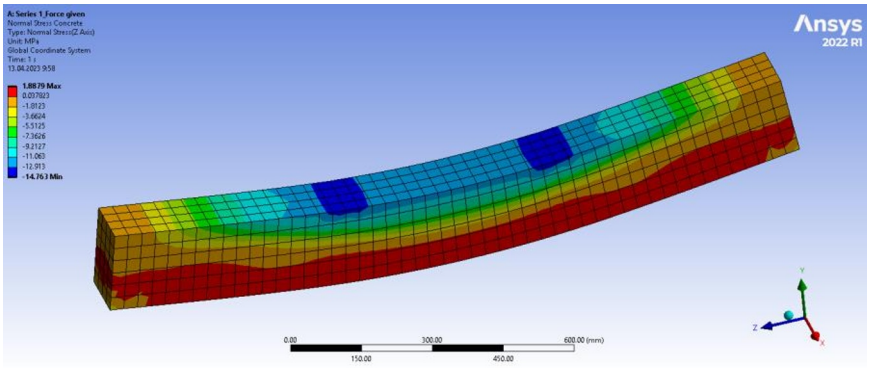

Fig. 5. Variation ranges of concrete stresses for Series 1, MPa

In Series 2 specimens, when subjected to a load of 50.8 kN, the stress in the reinforcement in the tensile zone reached the yield point, Figure 6. At the same time, failure of concrete in the tensile zone was observed. As a result of the installation of reinforcement in the compressive zone, the stresses of concrete in the compressive zone do not reach its limit strength σ_b=2.42 MPa, Fig. 7. The stress in the steel reinforcement in the compressive zone reached σ_s=83.029 MPa. It was observed that the strength of the concrete and rebar in the compressive zone was not used sufficiently because the failure started in the tensile zone.

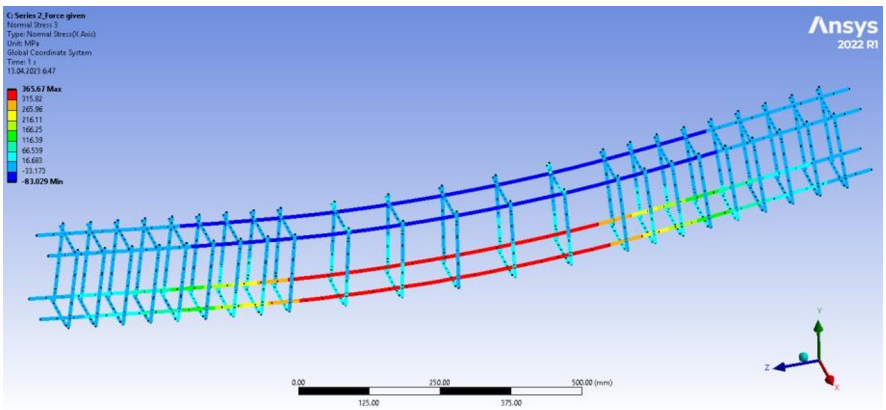

Fig. 6. Variation ranges of rebar stresses for Series 2, MPa

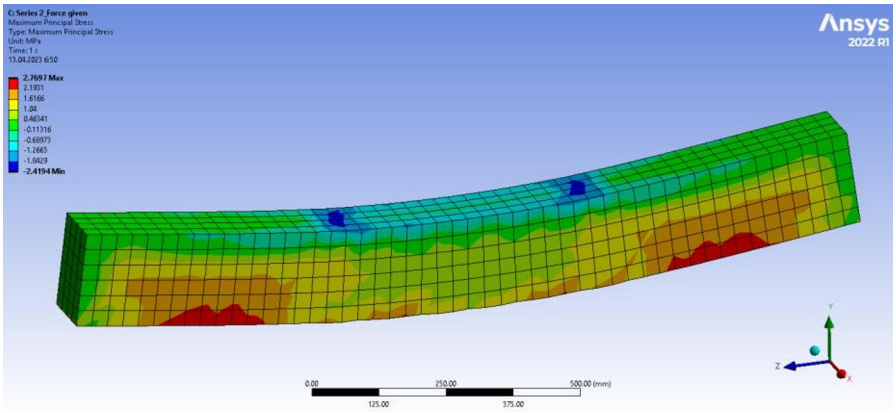

Fig. 7. Variation ranges of concrete stresses for Series 2, MPa

For Series 3, basalt composite reinforcement was placed in the compression zone and steel reinforcement in the tensile zone of the beam, and when it was subjected to an external load of 53 kN, it was found that the tensile rebar strength reached its yield point, Fig. 8. When the formation of concrete cracks in the tensile zone, BFRP stress in the compressive zone is equal to σ_s=44.04 MPa. Concrete stresses in the compressive zone were much smaller than their limit value (4.018 MPa), as shown in Fig. 9.

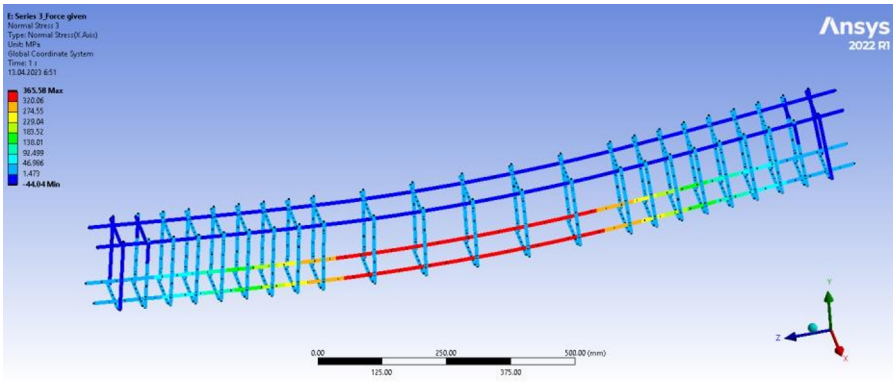

Fig. 8. Variation ranges of rebar stresses for Series 2, MPa

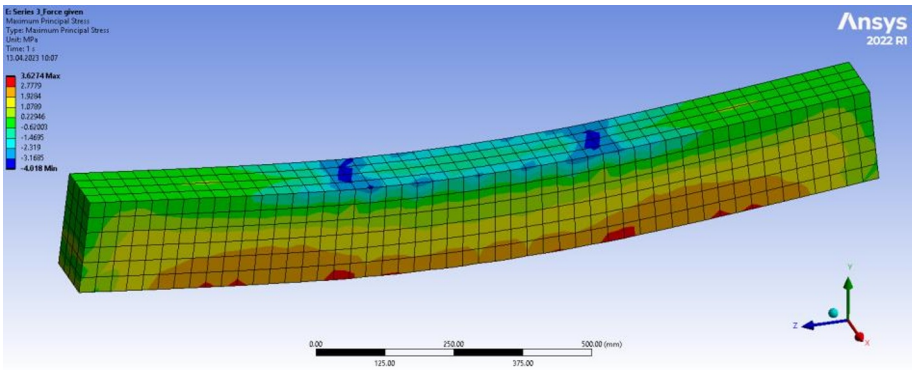

Fig. 9. Variation ranges of concrete stresses for Series 3, MPa

When a load is applied to the sample, the relationship interaction between load and deflection is manifested in a nonlinear curve depending on the properties of the concrete. As the percentage of reinforcement was normal, failure in all cases was characterized by reaching the yield strength of the rebar in the tensile zone and increasing stresses in the concrete and reinforcement bars in the compressive zone.

The load-deflection diagram for Series 1 is shown in Fig. 10 and compares experimental, theoretical, and ANSYS results to each other. Based on the diagram, it can be said that the value of the destructive force of the beam reaches the highest value as a result of the experiment, that is, 45.7 kN and the deflection is also the largest value in the experimental study, which is $f=6.08\ mm$, Fig. 10. The deflection limit value for the samples is $f_{ult}=l_0/150=9.6\ mm$.

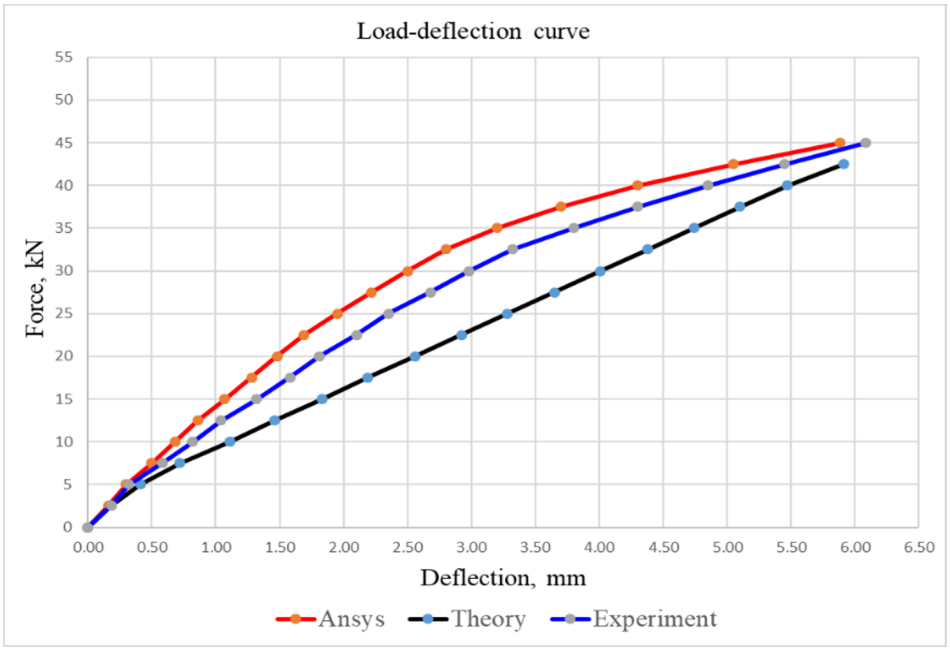

Fig. 10. Load-deflection curve for Series 1

In series 2, destructive force in ANSYS has the highest value of 50.8 kN, and deflection is 3.84 mm. As a result of the experiment, mid-span deflection is equal to 6.08 mm, which is the maximum value of Series 2 samples. In hand calculation, the maximum force is the smallest value (46.29 kN). The fact that the experimental line is in the middle of the other two results can be analyzed by looking at the diagram in Fig. 11.

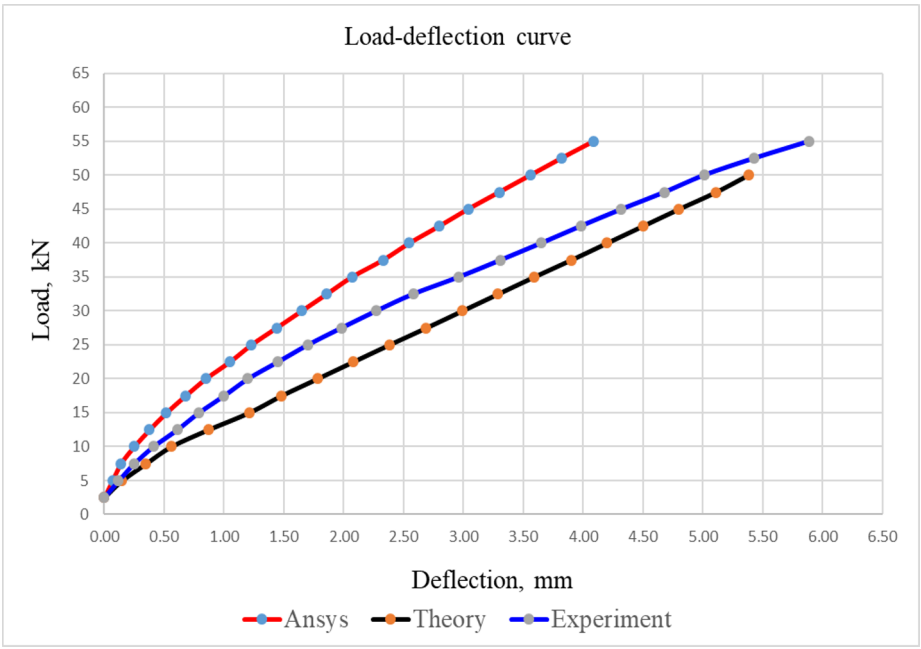

Fig. 11. Load-deflection curve for Series 2

Figure 12 shows the load-deflection diagram of Series 3 specimens, where the destructive force value obtained in ANSYS was 54 kN with a beam deflection of 4.38 mm. In the hand calculation, the maximum force value was the smallest, equal to 45.31 kN, and the deflection was 5.89 mm. It can be seen that the value obtained from the experiment is between the theoretical and the finite element line, and in this case, the mid-span deflection reaches its maximum value according to the diagram (6.31 mm).

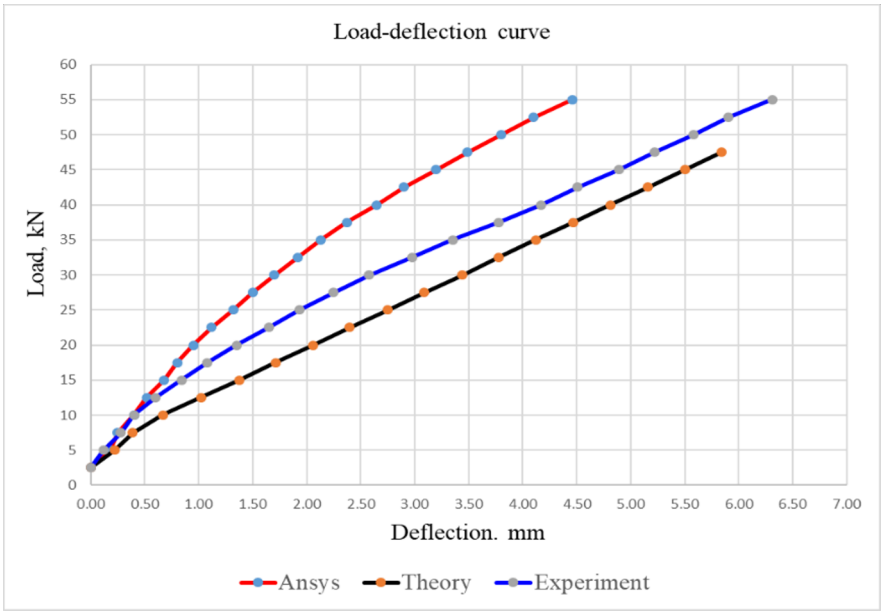

Fig. 12. Load-deflection curve for Series 3

4 Conclusions

In this article, the results were obtained by finite element modeling considering the nonlinear properties of concrete beams with combined reinforcement. The general conclusion of this study is outlined below.

1. In the case of an unreinforced compression zone, the strength of the tensile reinforcement bar and concrete is fully used, but it can be seen that its load-bearing capacity is lower than that of beams with compression zone reinforcement. The stresses generated in the concrete in the compressive zone are equal to σ_b=14.76 MPa for Series 1, σ_b=2.42 MPa for Series 2, and σ_b=4.018 MPa for Series 3. Rebar stresses in the compressive zone are σ_s=83.029 MPa for Series 2 and σ_s=44.04 MPa for Series 3. The value of the destructive force in the samples of Series 3 is 7.5% higher than that of the samples of Series 2, while the mid-span deflection is greater than that of Series 2 due to the higher value of the destructive force of Series 3.

2. Structural reinforcement bar installed in the compression zone, which is not considered in theoretical calculations, increases the strength of the structure by 12-18% due to the finite element method and experimental testing.

3. Using BFRP bar instead of steel reinforcement in the compressive zone increases the load-bearing capacity of the beam, saves steel consumption, and reduces the cost of the structure.

References

1. Mohamed A.A.El-Shaer. Structrual Analysis of Concrete Beams Reinforced with Basalt FRP Bars. IOSR Journal of Mechanical and Civil Engineering (IOSR-JMCE). No. 13, Volume 13, Issue 3 Ver. VI (May- Jun. 2016), PP 34-49
2. Rania Mohammed, Zhou Fangyuan. Numerical Investigation of the Behavior of Reinforced Concrete Beam Reinforced with FRP Bars. Civil Engineering Journal 5(11):2296-2308. DOI:10.28991/cej-2019-03091412
3. Barris C., Torres L., Turon A., Baena M., Mias C. Experimental study of flexural behaviour of GFRP reinforced. Fourth International Conference on FRP Composites in Civil Engineering (CICE2008). Zurich, Switzerland, 22–24 July 2008.
4. Barris C., Torres L., Comas J., Mias C. Cracking and deflections in GFRP RC beams: an experimental study. Composites: Part B, 55. 2013, pp. 580–590.
5. Barris C., Torres L., Turon A., Baena M., Mias C. Experimental study of flexural behaviour of GFRP reinforced // Fourth International Conference on FRP Composites in Civil Engineering (CICE2008). Zurich, Switzerland, 22–24 July 2008.
6. Pawłowskia D., Szumigałaa M. Flexural behaviour of full-scale basalt FRP RC beams – experimental and numerical studies. 7th Scientific-Technical Conference Material Problems in Civil Engineering (MATBUD'2015). Procedia Engineering 108. 2015, pp. 518–525.
7. Urbanski M., Garbacz A., Lapko A. Investigation on concrete beams reinforced with basalt rebars as an effective alternative of conventional R/C structures. Proceedings of the 11th International Conference on Modern Building Materials, Structures and Techniques. Procedia Engineering 57. 2013, pp. 1183–1191.
8. Frolov N.V. Experimental research of concrete beams with glass-plastic bars in tensioned area. Vestnik Belgorodskogo gosudarstvennogo tekhnologicheskogo universiteta im. V.G. SHuhova. 2016. No. 2, pp. 46–50. (In Russian).

9. Zhu, Haitang, Shengzhao Cheng, Danying Gao, Sheikh M. Neaz, and Chuanchuan Li. "Flexural Behavior of Partially Fiber-Reinforced High-Strength Concrete Beams Reinforced with FRP Bars." Construction and Building Materials 161 (February 2018): 587–597. doi:10.1016/j.conbuildmat.2017.12.003.
10. Alsayed, Saleh H., and Abdulrahman M. Alhozaimy. "Ductility of Concrete Beams Reinforced with FRP Bars and Steel Fibers." Journal of Composite Materials 33, no. 19 (October 1999): 1792–1806. doi:10.1177/002199839903301902.
11. Antakov I.A. Features of Behavior of Flexural Members with Composite Polymeric Reinforcement under Load. Nauchno-texnicheskiy i proizvedstvenniy jurnal. 2018. No. 5, pp. 15-18. (In Russian)
12. Rakhmonov A.D., Solov'ev N.P., Pozdeev V.M. Komp'yuternoe mod-elirovanie dlya issledovaniya napryazhenno-deformirovannogo sostoyaniya balok s kom-binirovannym armirovaniem [Computer Modeling for Investigating Stress-strain State of Beams with Hybrid Reinforcement]. Vestnik MGSU [Proceedings of Moscow State University of Civil Engineering]. 2014, no. 1, pp. 187—195.
13. Begunova N.V., Grahov V.P., Vozmishchev V.N., Kislyakova I.G. Comparative Evaluation of Results on Test of Concrete Beams with Fiberglass Rebar and Calculated Data. Science & Technique. 2019;18(2):155-163. (In Russ.) https://doi.org/10.21122/2227-1031-2019-18-2-155-163
14. Garbacz A, Lapko A, Urbanski M. Investigation on concrete beams reinforced with basalt rebars as an effective alternative of conventional R/C structures. Proceedingos f the 11 th International Conference on Modern Building Materials, Structures and Techniques. Procedia Engineering 2013;57: p.1183-1191.
15. ACI Guide for the design and construction of structural concrete reinforced with FRP bars. ACI 440.1R-06, American Concrete Institute, 2006.
16. Fib Bulletin 40/2007. FRP Reinforcement in RC structures, technical report. International Federation for Structural Concrete (fib). September 2007, p. 3-30.
17. Babych Y. M. et al. Results of experimental research of deformability and crack-resistance of two span continuous reinforced concrete beams with combined reinforcement //IOP Conference Series: Materials Science and Engineering. – IOP Publishing, 2019. – Т. 708. – №. 1. – С. 012043.
18. Yang, Y., Pan, D., Wu, G., & Cao, D. (2021). A new design method of the equivalent stress–strain relationship for hybrid (FRP bar and steel bar) reinforced concrete beams. Composite Structures, 270, 114099.
19. Slaitas, J., Valivonis, J., & Rimkus, L. (2020). Evaluation of stress-strain state of FRP strengthened RC elements in bending. Fracture mechanics approach. Composite Structures, 233, 111712.
20. Najaf, E., Orouji, M., & Ghouchani, K. (2022). Finite element analysis of the effect of type, Number, and Installation Angle of FRP Sheets on improving the Flexural Strength of Concrete Beams. Case Studies in Construction Materials, 17, e01670.
21. Amin, M. N., Iqbal, M., Khan, K., Qadir, M. G., Shalabi, F. I., & Jamal, A. (2022). Ensemble tree-based approach towards flexural strength prediction of frp reinforced concrete beams. Polymers, 14(7), 1303.
22. Murad, Y., Tarawneh, A., Arar, F., Al-Zu'bi, A., Al-Ghwairi, A., Al-Jaafreh, A., & Tarawneh, M. (2021, October). Flexural strength prediction for concrete beams reinforced with FRP bars using gene expression programming. In Structures (Vol. 33, pp. 3163-3172). Elsevier.

23. Yoon, Y. S., Yang, J. M., Min, K. H., & Shin, H. O. (2011). Flexural strength and deflection characteristics of high-strength concrete beams with hybrid FRP and steel bar reinforcement. Special Publication, 275, 1-22.
24. Buyukozturk, O., & Hearing, B. (1998). Failure behavior of precracked concrete beams retrofitted with FRP. Journal of composites for construction, 2(3), 138-144.
25. Lau, D., & Pam, H. J. (2010). Experimental study of hybrid FRP reinforced concrete beams. Engineering Structures, 32(12), 3857-3865.
26. Kim S., & Kim S. (2019). Flexural behavior of concrete beams with steel bar and FRP reinforcement. Journal of asian architecture and building engineering, 18(2), 89-97.